Treatment of dairy wastewater by graphene oxide nanoadsorbent and sludge separation, using In Situ Sludge Magnetic Impregnation (ISSMI)

Falahati, F., Baghdadi, M.[*] and Aminzadeh, B.

Department of Environmental Engineering, Graduate Faculty of Environment,
University of Tehran, Tehran, Iran

ABSTRACT: The present research investigates the ability of graphene oxide nanosheets for treatment of dairy wastewater, using In Situ Sludge Magnetic Impregnation" (ISSMI) to separate sludge after adsorption process. To increase the interaction between magnetic nanoparticles and graphene oxide, the former has been functionalized, using 3-Aminopropyl triethoxysilane, with the synthesized graphene oxide and magnetic nanoparticles being characterized by FT-IR, SEM, and NCHS analysis. The experiments have been conducted on the effluent of Pegah factory. The batch adsorption experiments have been carried out to investigate the effect of adsorbent dose, contact time, and pH on the removal of total nitrogen, total phosphorus, COD, and turbidity. At adsorbent dose of 320 mg L^{-1}, the removal efficiencies of 90, 80, 84, and 94% have been observed for TN, TP, COD, and turbidity, respectively. The adsorbent data has been modeled by Langmuir and Freundlich isotherms, giving results that are compatible with Freundlich isotherm. TN, TP, and COD are mostly particulate materials in dairy wastewaters; therefore, when nanosheets aggregate, particulate materials are trapped between GO nanosheets; as a result, pollutants are distributed heterogeneously on the adsorbent's surface. Consequently, adsorption does not occur as monolayer on the surface of GO; for this reason, adsorption follows Freundlich model. Maximum absorption capacity of the adsorbent turns out to be 730 mg g^{-1} for total nitrogen, 600 mg g^{-1} for total phosphorus, 26000 mg g^{-1} for COD, and 5500 mg g^{-1} for turbidity. Adsorption kinetic has been studied with the first and second order equation, giving results that are compatible with second order equation.

Keywords: adsorption, dairy wastewater, graphene oxide, magnetic nanoparticles, removal.

INTRODUCTION

Dairy industry generates highly-polluted wastewater, characterized by high Biological Oxygen Demand (BOD), Chemical Oxygen Demand (COD), Total Suspended Solids (TSS), oil and grease content, high nutrient levels, organic compounds, and pathogens (Porwal et al., 2015). Properties of raw dairy wastewater vary, depending on produced food and production technologies (Särkkä et al., 2015). For instance, the wastewater from milk processing has a COD level around 3000 mg L^{-1} whereas this value can reach 50,000 mg L^{-1} during the production of cheese (Gavala et al., 1999). Conventional dairy wastewater treatment fails when high amounts of proteins and lipids are present,

[*] Corresponding author, Email: m.baghdadi@ut.ac.ir

causing some problems, such as alkaline pH, color change, and high levels of both COD and BOD (Drogui et al., 2008). Dairy industry pollution is mostly of an organic source, and all processes in the production chain, including manufacturing, packaging, transportation, and storage affect the environment (Kushwaha et al., 2011). Nitrogen sources in dairy wastewater are organic nitrogen comprising urea and nucleic acids, as well as ions like NH_4^+, NO_2^-, and NO_3^-. Sources of phosphorus in milk wastewater are mainly inorganic compounds, such as orthophosphates and polyphosphates, produced form organic compounds (Demirel et al., 2005).

Wastewaters with high organic content cause lots of ecological problems. Discharge of untreated wastewater to the land alters physical and chemical properties of soil, while its discharge to water bodies may result in eutrophication, making water unfit for drinking (Manu et al., 2011). It also causes toxicity for aquatic organisms and reduces dissolved oxygen (Rahimi et al., 2011). Phosphorus is one of the major factors, increasing algae growth; however, combined with nitrogen, it causes serious eutrophication problems in lakes, rivers, and seas (Mañas et al., 2011). Different biological treatments have been used for dairy wastewater, e.g. activated sludge process (Tawfik et al., 2008), anaerobic lagoon, aerobic lagoon, combined trickling filter system, etc. (Gavala et al., 1999).

One of the widely used methods is chemical treatment of dairy wastewater, employed in various processes, such as electrocoagulation (Yavuz et al., 2011), advanced Fenton, and photo-Fenton methods (Loures et al., 2013). Membrane processes (Luo et al., 2011), natural evaporation, and adsorption can also be referred to as physical methods to treat dairy wastewaters. Natural, low-cost adsorbents have been used to remove organic materials from dairy wastewaters, though some of the most-used adsorbents for this purpose are activated carbon powder, bagasse ash (Kushwaha et al., 2010), fruit wastes, coconut shell, etc. (Ali et al., 2012).

Graphene Oxide (GO), a nanostructure with oxygen functional groups and SP_2 aromatic rings, can be involved in a wide range of interactions and show interesting properties in areas like pharmacology, energy storage, and water and wastewater purification. GO can adsorb a wide range of contaminants belonging to various functional groups, such as epoxy (C-O-C), hydroxyl (OH), and carboxyl groups (COOH) (Omidinia et al., 2013). GO is obtained through oxidation of graphite powder by strong oxidants. The specific surface area of GO is 2630 m/g (Zhu et al., 2010); as a result, it can adsorb high amounts of pollutants in.its surface.

High dispensability and small particle size are considered drawbacks of GO, making it difficult to separate after adsorption. For this reason, magnetic nanocomposite of graphene oxide has been reported as a useful alternative that can be separated easily with a magnet. However, the adsorption capacity of GO, incorporated in nanocomposite, decreases since its active sites are blocked by magnetic nanoparticles, subsequently decreasing its surface area (Moharramzadeh & Baghdadi, 2016). The best way is to add nonmagnetic graphene oxide and magnetic nanoparticles to wastewater, resulting in magnetic sludge that can be easily separated by a magnet. In this regard, In Situ Sludge Magnetic Impregnation" (ISSMI) has been reported not only for using maximum adsorption capacity of GO but for increasing the amount of sludge sedimentation and decreasing sludge volume (Moharramzadeh & Baghdadi, 2016).

This research has investigated the ability of graphene oxide nanosheets to treat dairy wastewater, in which application of In Situ Sludge Magnetic Impregnation" (ISSMI) has been studied for sludge separation after adsorption process.

MATERIALS AND METHODS

$FeCl_2.4H_2O$, $FeCl_3.6H_2O$, polyethylene glycol (PEG), ammonia (25% w/w), ethanol, tetraethyl orthosilicate (TEOS), and 3-Aminopropyl) triethoxysilane (APTMS), all used to prepare magnetic nanoparticles, were purchased from Merck company (Darmstadt, Germany). Graphene oxide was synthesized from Graphite fine powder, obtained from LOBA Chemie (India), while sulfuric acid (98% w/w), sodium nitrate, potassium permanganate, hydrogen peroxide (30% w/w), and hydrochloric acid (37% w/w), also used for preparing GO, were obtained from Merck company, as well.

In this study, wastewater was taken from influent of primary sedimentation basin of wastewater treatment plant at Pegah dairy company (Milk Production Plant, Tehran, Iran). Table 1 gives the traits of this wastewater.

Table 1. Analysis of wastewater effluent*

Parameter	Unit	Quantity
BOD	mg L^{-1}	1800
COD	mg L^{-1}	4000
TN	mg L^{-1}	100
TP	mg L^{-1}	88
Turbidity	NTU	461

*Taken from the influent primary sedimentation basin of wastewater treatment plant

The amounts of COD, total nitrogen (TN), and total phosphorus (TP) were measured, using a spectrophotometer (DR 5000 and HACH), while the sample's turbidity was measured with a turbidimeter (Hach Company, Loveland, Colo) and pH measurement was done via a pH-meter (Metrohm 691, Sweetzerland). An ultrasonic bath was used to disperse the nanoparticles

Graphene oxide was prepared from natural graphite powder, based on modified Hummer's method (Hummers & Offeman, 1958). In order to prevent oxidation and aggregation of nanoparticles, their surface was reformed by silica. Generally, compounds, covered by silica, have an excellent biocompatibility and a high solubility in a wide range of pH (Khosroshahi & Ghazanfari, 2012). To increase the interaction between the magnetic nanoparticles and graphene oxide, surface of the magnetic nanoparticles was modified with amine functional group. Amino functionalized magnetic nanoparticles were synthesized according to several studies (Zong et al., 2013; Khosroshahi & Ghazanfari, 2012).

Magnetization measurement of magnetite nanoparticles was carried out, using a Vibration Sample Magnetometer (VSM) with an applied magnetic field of -10000 to 10000 Oersted. FTIR spectra of graphene oxide and $Fe_3O_4@SiO_2-NH_2$ magnetic nanoparticles were recorded on a FT-IR spectrometer (Bruker, Tensor 27, Germany) with KBr pellets being within the range of 4000-400 cm^{-1}. The morphological studies were conducted by field emission scanning electron microscope (FESEM, Hitachi, S4160, Japan).

Experiments on batch adsorption were conducted to investigate the effect of adsorbent dose, the contact time, and pH on TN, TP, and COD removal as well as turbidity from dairy wastewater. The effect of GO, pH, and contact time were studied in the range of 80-480 mg L^{-1}, 2-10, and 1-25 min, respectively. Absorption kinetics were evaluated, using pseudo-first and second order models. In order to determine the adsorption isotherm, batch adsorption experiments were conducted in which solutions with different concentrations of nitrogen and phosphorus were exposed to constant absorbed dose. Figure 1 represents the performance of graphene oxide and magnetic nanoparticles in treatment of dairy wastewater and separation of sludge, using ISSMI process.

DISCUSSION AND RESULTS

SEM images, presented in Figure 2, illustrate the morphology of graphene oxide, showing particles with sheet structure. The particles' size was estimated to be below 1 μm. Figure 3 shows FT-IR

analysis of graphene oxide. O-H bonds, referring to hydroxyl groups, were observed within the range of 3400-3600 cm^{-1}. C-H, C=O, C=C, and C-O bonds were observed in the ranges of 3000-3200 cm^{-1}, 1700-1800 cm^{-1}, 1600-1650 cm^{-1}, and 950-1050 cm^{-1}, respectively, which is in accordance with previous results. CHNS analysis was used to determine nitrogen, carbon, hydrogen, sulfur, and oxygen in GO, which were 0.00, 36.85, 1.34, 0.32, and 61.50%, respectively, confirming graphite oxidation.

Fig. 1. Performance of Graphene oxide and magnetic nanoparticles in treatment of dairy wastewater and separation of its sludge using a magnet
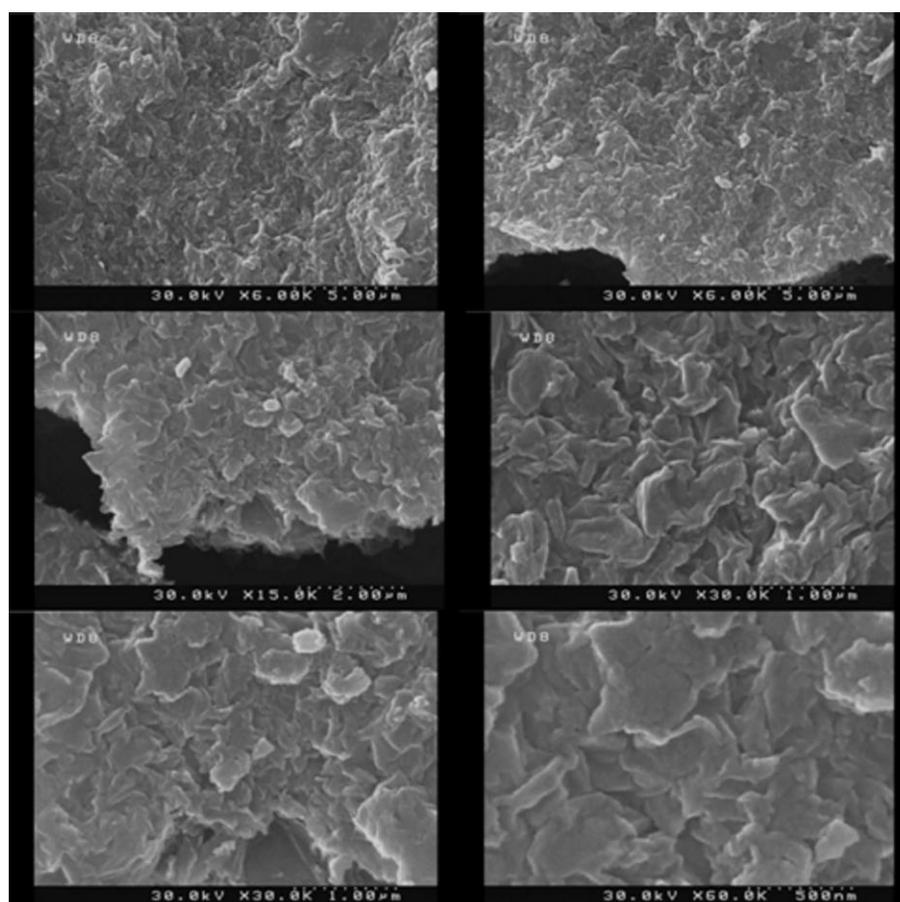
Fig. 2. FESEM images of Graphene oxide
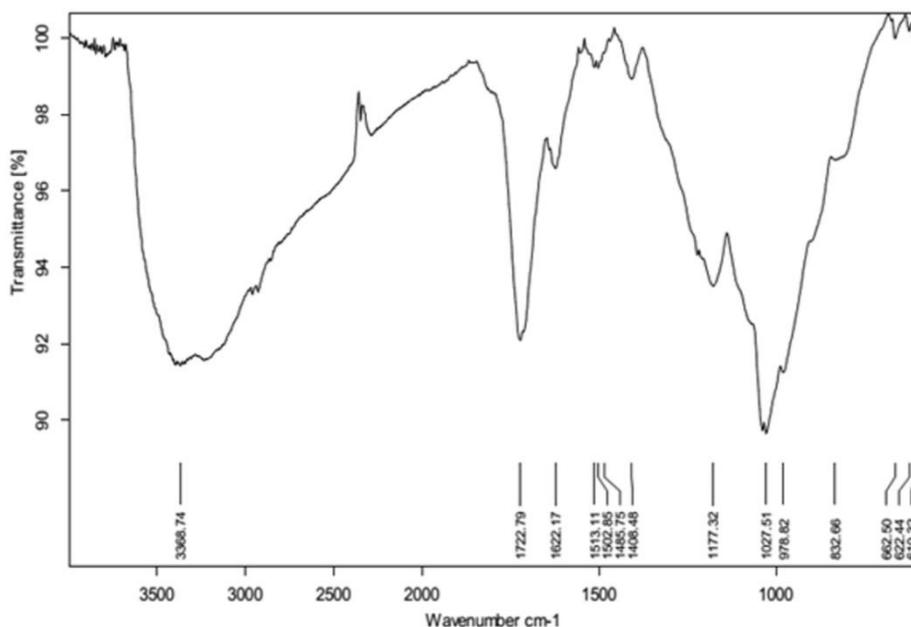
Fig. 3. FT-IR spectra of Graphene oxide

Figure 4 illustrates SEM images of $Fe_3O_4@SiO_2-NH_2$. Clearly, the particles' size is less than 100 nm. The magnetic feature of $Fe_3O_4@SiO_2-NH_2$ particles was measured via induction of a magnetic field with a vibration sample magnetometer (VSM). Figure 5a shows the magnetization curve of magnetic nanoparticles under a magnetic field of -10000 to 10000 Oersted. As it can be seen, no magnetic hysteresis loop was observed in the curve, confirming the super-paramagnetic feature of this compound with enough magnetic saturation of 30 emu/g to be separated, using a magnet Figure 5b.
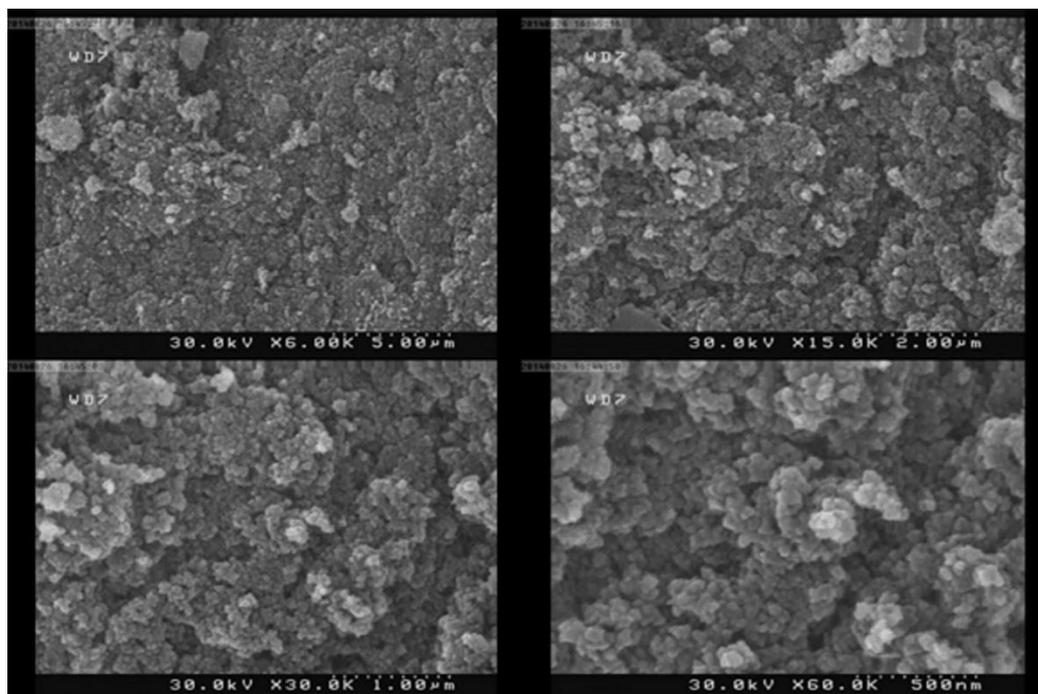
Fig. 4. FESEM images of $Fe_3O_4@SiO_2-NH_2$
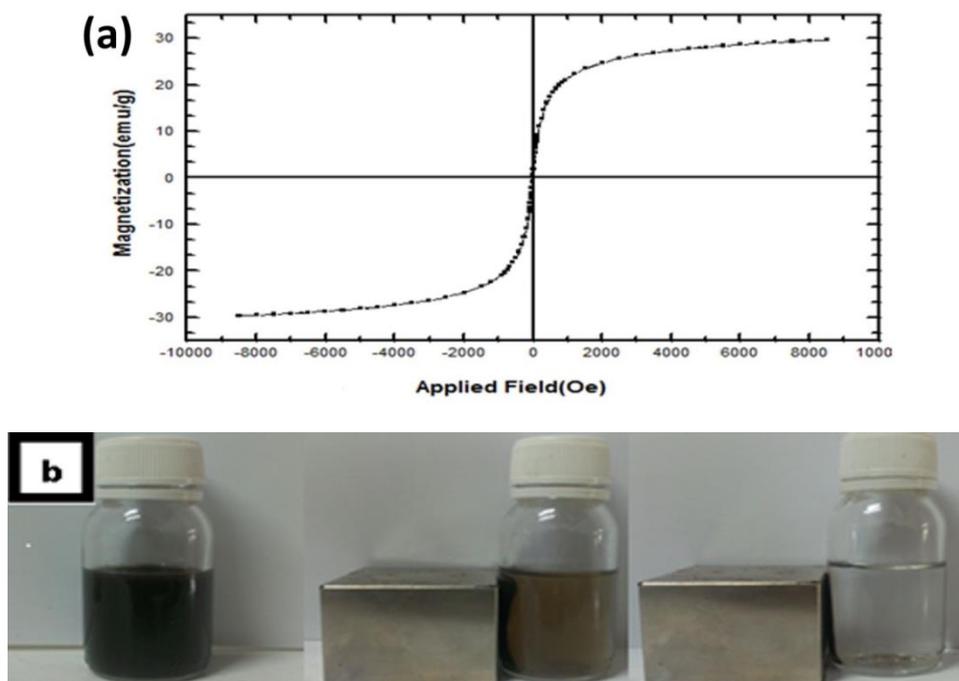
Fig. 5. (a) magnetic measurement data of Fe3O4@SiO2-NH2, (b) effect of external magnetic field on separating nanoparticles from solution

The effect of adsorbent dose on TN and TP removal was assessed. Stock suspensions of GO (2000 mg L^{-1}) and magnetic nanoparticles (4000 mg L^{-1}) were prepared. They were placed in the ultrasonic bath for 30 min. The experiments were all carried out at the wastewater pH, equal to 7. Initially, 2 mL of magnetic nanoparticles were added to 50 mL of samples while being stirred. Then GO was added and stirred for 30 minutes. The created magnetic sludge was separated by placing it on a magnet. Treated wastewater was evaluated to measure TN, TP, COD, and turbidity, with its results demonstrated in Figure 6. As can be seen, by increasing GO dose, TN, TP, COD, and turbidity decreased significantly.

According to Figures 6a and 6b, the highest nitrogen and phosphorous removal efficiency were 88% and 77%, respectively at absorbent dose of 480 mg L^{-1}. To decrease the adsorbent consumption, adsorbent dose of 160 mg L^{-1} was chosen as the optimum point, in which removal efficiencies for TN and TP were 85% and 74%, respectively. It should be noted that

the initial TN and TP concentration in wastewater were 100 and 87.9 mg L^{-1}, respectively. According to Figure 6c, by increasing the amount of absorbent, COD removal increased, as well. After the dose of 160 mg L^{-1}, the diagram slope decreased. The highest rate of COD removal was 86% at a dose of 480 mg L$^{-1.}$ Removal efficiency at the dose of 160 mg L^{-1} was 84%, which was chosen as the optimal dose. COD of raw sewage was 4000 mg L^{-1}.

According to Figure 6d, the removal efficiency of wastewater turbidity ranged between 86.1% at dose of 80 mg L^{-1} and 98.5% at dose of 400 mg L^{-1}. In order to remove the three previous parameters (TN, TN, and COD), the adsorbent dose of 160 mg L^{-1} was selected as the optimal one, at which the removal efficiency of turbidity removal was 94.14%. The turbidity of raw sewage was 461FTU. According to the results of the effect of adsorbent dose, it can be concluded that by increasing the amount of adsorbent removal efficiency of the studied parameters rose due to the increase in the number of active sites.
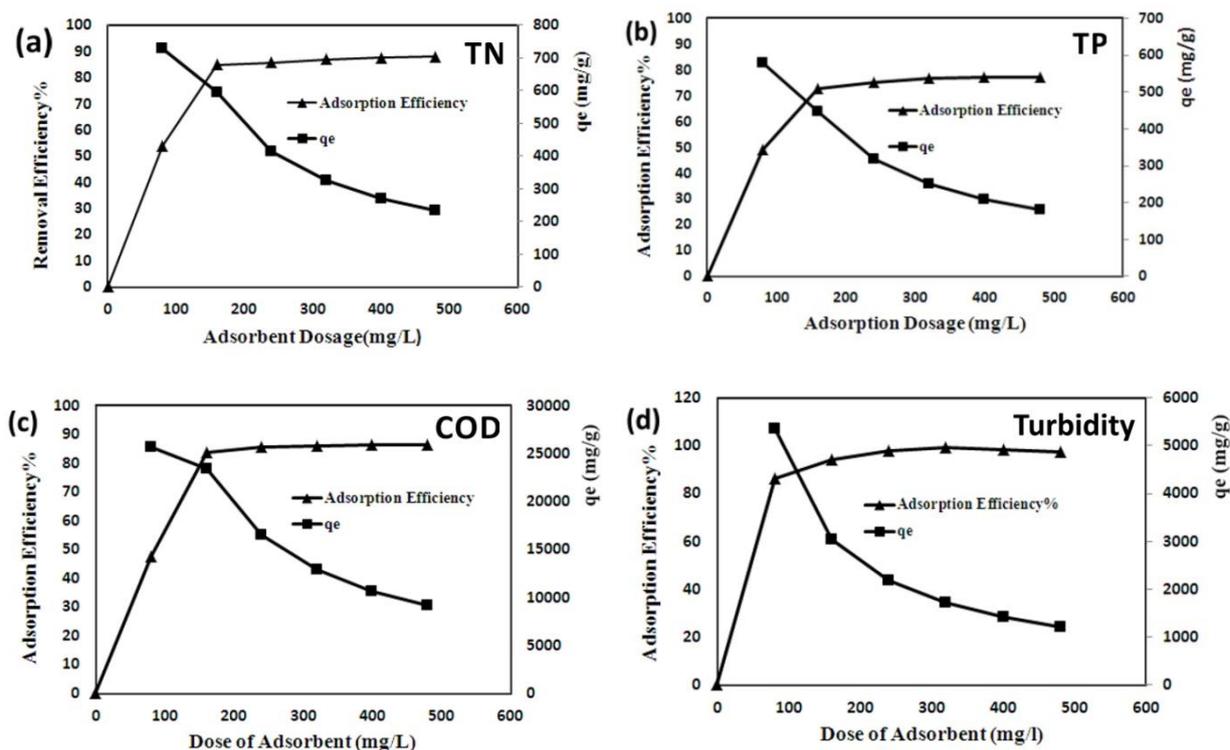
Fig. 6. Effect of adsorbent dose on (a) TN, (b) TP, (c) COD, and (d) turbidity removal

The impact of pH was investigated in the range of 2 to 12. In order to adjust pH, sulfuric acid and sodium hydroxide solutions (1 mol L^{-1}) were used. Figures 7a and 7b demonstrate the results of TN and TP removal, respectively, indicating that TN and TP removal rose by increasing pH. At low pH, the surface charge of graphene oxide reduces and graphene oxide nanosheets can stick together; as a consequence, the specific surface area decreases. The highest removal efficiencies of 88% and 78% were obtained for TN and TP at pH level of 8.8, respectively. The subsequent experiments were performed at sewage pH, equal to 7. Removal efficiencies of nitrogen and phosphorous at this pH were 82% and 76.4%, respectively.

Regarding Figure 7c, efficiency of COD removal increased from 73.8% at pH = 2 to 86.3% at pH = 12, and at the pH of raw sewage, removal efficacy was 86%. As shown in Figure 7d, sewage turbidity removal efficiency was 91% at pH = 2, reaching its highest amount of 98% at pH = 8.

This section presents the effect of contact time on the performance of graphene oxide in decreasing nitrogen and phosphorus, COD, and sewage turbidity. The contact time between 1 and 30 min was selected for this purpose; and the results are shown in Figure 8 By increasing the contact time, the removal efficiency of TN, TP, COD, and turbidity increased. The highest removal efficiencies were obtained after 10 min of stirring (81% for TN, 81% for TP, 86% for COD, and 92% for turbidity). Approximately, removal efficiencies of 80%, 77%, 82%, and 90% were observed for TN, TP, COD, and turbidity, respectively after 5 min; indicating the high rate of adsorption process.
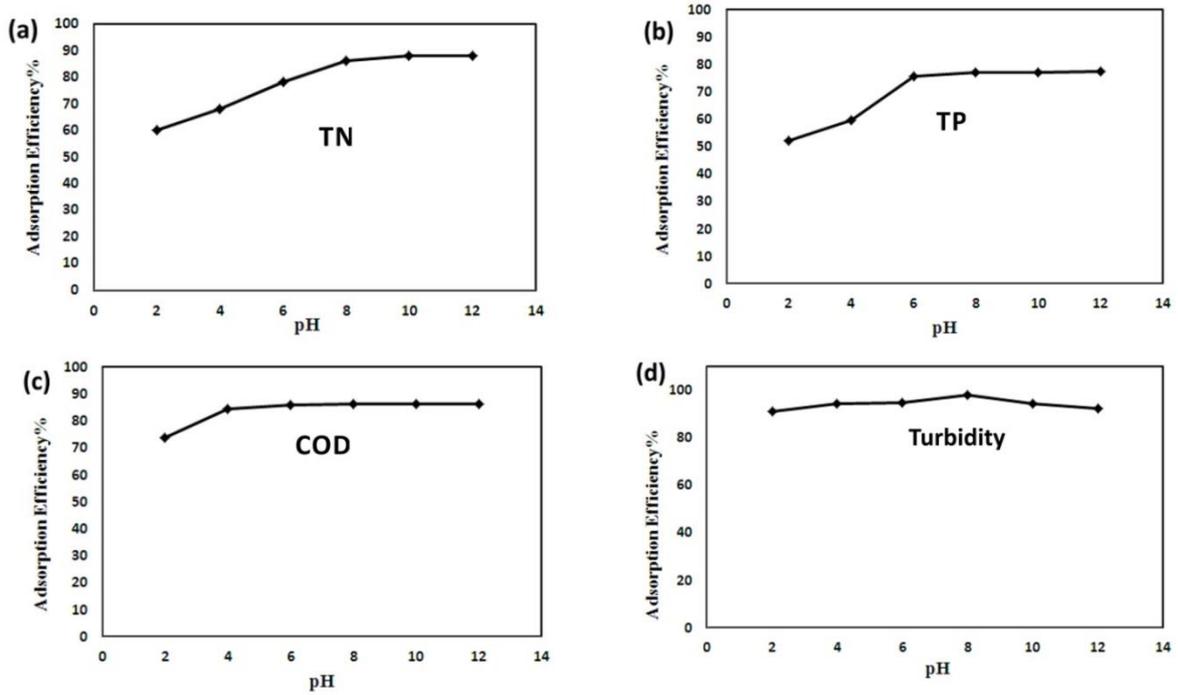
Fig. 7. Effect of pH on (a) TN, (b) TP, (c) COD, and (d) turbidity removal
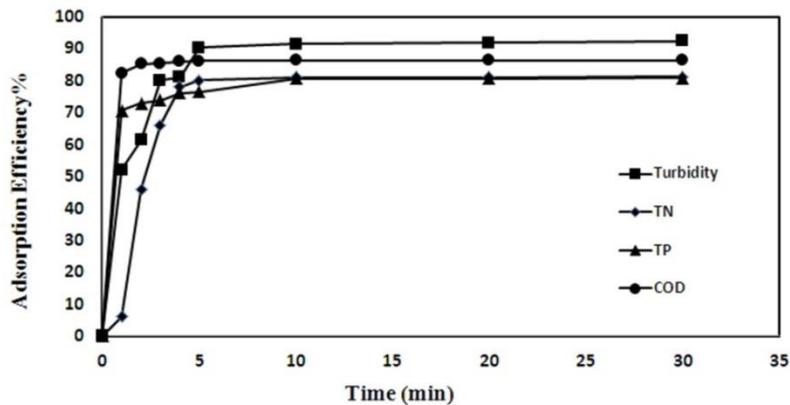
Fig. 8. Effect of contact time on TN, TP, COD, and Turbidity removal

The adsorption isotherm indicates the relation between the equilibrium concentration of the pollutant in solution (C_e) and in adsorbent (q_e). Absorption data were analyzed by three well-known models: Langmuir, Freundlich, and Temkin.

Langmuir Model considers the mono layer adsorption on identical active sites of adsorbent without any interaction between the adsorbed molecules (Doğan et al., 2000). It is able to estimate the maximum adsorption capacity adsorbent corresponding to monolayer adsorption on the surface of adsorbent. However, Freundlich is based on multi-layer adsorption process (Kurniawan et al., 2012), whereas Temkin isotherm assumes that the heat of adsorption of all molecules decreases linearly with coverage, due to adsorbent–adsorbate interaction. The adsorption is characterized by a uniform distribution of binding energies (Hameed, 2009). In order to calculate adsorption isotherms, the sewage was diluted, using deionized water to obtain samples with different concentrations of TN, TP, COD, and turbidity. The equilibrium experiments

were conducted at the optimum condition. Table 2 present the linear forms of the models. The equilibrium adsorption of TN, TP, COD, and turbidity by GO was investigated through the mentioned isotherms, its results presented in Table 2.

The residual root-mean-square error (RMSE), average absolute relative error (AARE), and the chi-square test (χ2), were used to evaluate the agreement between the experimental data and predictions using models. The related equations are as follow:

$$RMES = \sqrt{\frac{1}{n-p}\sum_{i=1}^{n}\left(q_{e,\,exp} - q_{e,\,cal}\right)_i^2} \qquad (1)$$

$$AARE = \frac{1}{N}\sum_{i=1}^{N}\left[\left|\frac{(q_{e,cal} - q_{e,exp})}{q_{e,exp}}\right|\right]_i \qquad (2)$$

$$\chi^2 = \sum_{i=1}^{n}\left[\frac{\left(q_{e,exp} - q_{e,cal}\right)^2}{q_{e,cal}}\right]_i \qquad (3)$$

where $q_{e,\,exp}$ is the experimental results; $q_{e,\,cal}$, the calculated values using the model; n, the number of experimental data; and p, the number of model parameters. RMSE and AARE should be as small as possible. When more than one model is acceptable

statistically, the chi-square (χ^2) test is required to find the best-fit model. The lowest value indicates the best model (Mitra et al., 2014).

The performance of different models was evaluated by error functions and its results are shown in Table 3. According to RMSE, AARE, and χ2 values, Freundlich and Temkin exhibited lower errors than Langmuir. The fitting degree followed the sequence: Freundlich> Temkin > Langmuir. Owing to the low determination coefficients of Langmuir isotherm, this model is not valid for description of q_{max}; as a consequence, q_{max} obtained from this model were not in agreement with the experimental data. In the wastewater, TN, TP, and COD were mostly as particulate materials; therefore, when the GO nanosheets aggregated, particulate materials were trapped between nanosheets. As a consequence, the adsorption did not occur as monolayer on the surface of GO. For this reason, the adsorption followed Freundlich model. Table 4 gives the maximum adsorption capacities of various adsorbents for all studied parameters. The adsorbent, used in the present study, showed excellent adsorbent capacities in comparison with other adsorbents.

Table 2. Isotherm parameters, obtained with linear regression for adsorption of TN, TP, COD, and turbidity, using GO

Isotherm	Equation		Parameters	TN	TP	COD	Turbidity
Langmuir	$\frac{C_e}{q_e} = \frac{1}{K_L q_m} + \frac{C_e}{q_m}$	(4)	q_m : mg L^{-1}	11.3	137	2500	333
			K_L : L mg^{-1}	0.080	0.017	0.002	0.014
Freundlich	$\ln q_e = \ln K_F + \frac{1}{n_F}\ln C_e$	(5)	$1/n_F$	3.650	1.350	2.067	1.904
			K_F : (mg g^{-1})(L mg^{-1})$^{1/n}$	0.025	1.369	0.029	0.516
Temkin	$q_e = B_1 \ln A + B_1 \ln C_e$	(6)	B_1 : mg g^{-1}	245.0	64.6	6902	738
			A : L mg^{-1}	0.283	0.257	0.008	0.076

q_m: maximum adsorption capacity reflected a complete monolayer (mg g^{-1}), K_L: Langmuir constant or adsorption equilibrium constant (L mg^{-1}), $1/n$: isotherm constant indicating the empirical parameter, K_F: isotherm constant indicating the capacity parameter (mg g^{-1})(L mg^{-1})$^{1/n}$, B_1: Temkin constant (mg g^{-1}), A: Temkin constant (L mg^{-1})

Table 3. ?

Models	TN				TP			
	R^2	RMSE	AARE	χ^2	R^2	RMSE	AARE	χ^2
Langmuir	0.740	210.3	0.813	30919	0.599	81.1	0.476	541.0
Freundlich	0.992	31.0	0.125	15.5	0.992	11.5	0.101	4.2
Temkin	0.824	116.4	3.019	294.6	0.885	26.6	0.946	-3.3
Models	COD				Turbidity			
	R^2	RMSE	AARE	χ^2	R^2	RMSE	AARE	χ^2
Langmuir	0.852	7654	0.603	190483	0.763	871.3	0.631	20654
Freundlich	0.992	562.0	0.999	245.8	0.994	122.0	0.086	48.0
Temkin	0.836	2288	1.351	-245.7	0.841	256.4	0.927	36.2

Table 4. Comparison of results with similar works

Type of wastewater	Pollutant	Adsorbent	Adsorption capacity(mg/g)	% Removal of pollutant	References
Artificial dairy	COD	Activated carbon	130	–	Kushwaha et al. (2010)
Artificial dairy	COD	Baggas fly ash	110	–	Kushwaha et al. (2010)
Dairy	COD	coconut shell activated carbon	–	75.3	Karale and Suryavanshi (2014)
Dairy	COD	Chitosan	–	79	Geetha Devi et al. (2012)
Dairy	Turbidity	Chitosan	–	93	Geetha Devi et al. (2012)
Dairy	COD	Carbon nanotube	–	81	Moradi and Maleki (2013)
Dairy	TN	Carbon nanotube	–	93	Moradi and Maleki (2013)
Dairy	COD	Biosorbent	–	65.4	Murali et al. (2013)
Dairy	COD	Graphene oxide	26000	84	Present study
Dairy	TN	Graphene oxide	730	90	Present study
Dairy	TP	Graphene oxide	600	80	Present study
Dairy	Turbidity	Graphene oxide	5500	94	Present study

Kinetics studies were carried out, using pseudo-first-order and pseudo-second-order models (Weber & Morris, 1963). The linear forms of the investigated models and the obtained results are presented in Table 5. Reliability of these kinetic models was determined by residual root-mean-square error (RMSE), average absolute relative error (AARE), and chi-square test (χ^2), with the results shown in Table 6. As it is shown, the regression coefficients (r^2) for pseudo-first-order model are too low and adsorption capacities calculated from pseudo-first-order model were significantly different from the experimental q_e. Thus, it is clear that the adsorption of all parameters on GO does not follow pseudo-first-order model. In pseudo-second-order model, the calculated adsorption capacities were close to experimental q_e. Therefore, it was concluded that the adsorption kinetics followed pseudo-second-order model; therefore, adsorption rate depended on both adsorbent dose and pollutant concentration. Figure 9 demonstrates the experimental and corresponding calculated data, using kinetic models, confirming the results of error analysis.

Table 5. Adsorption kinetic parameters, calculated by kinetic models for adsorption of TN, TP, COD, and turbidity, using GO

Model		Parameters	TN	TP	COD	Turbidity
Pseudo-first-order		k_1: min^{-1}	0.064	0.048	0.072	0.073
$\log(q_e - q_t) = \log(q_e) - \dfrac{k_1 t}{2.303}$	(7)	q_e (calc): mg g^{-1}	3.648	2.939	9.031	10.173
Pseudo-second-order		k_2: g mg^{-1} min^{-1}	0.001	0.019	0.002	0.001
$\dfrac{t}{q_t} = \dfrac{1}{k_2 q_e^2} + \left(\dfrac{1}{q_e}\right) t$	(8)	q_e (calc): mg g^{-1}	317	267.2	12978	1619

k_1: Rate constant of pseudo-first order adsorption (min^{-1}), k_2: second-order rate constant of adsorption (g mg^{-1} min^{-1}), q_e (calc): equilibrium capacity (mg g^{-1})

Table 6. ?

Model	Error Function	TN	TP	COD	Turbidity
Pseudo-first-order	R^2	0.5631	0.6392	0.8272	0.8460
	RMSE	300	282	14371	1612
	AARE	0.995	0.997	1.000	0.997
	χ^2	1069475	2543356	923452613	12386470
Pseudo-second-order	R^2	0.9840	1.000	1.000	1.000
	RMSE	58.80	4.81	60.59	93.90
	AARE	0.404	0.013	0.002	0.045
	χ^2	184.91	0.86	2.33	64.66

CONCLUSION

This research dealt with the dairy wastewater treatment by graphene oxide nanosheets. For this purpose, dairy wastewater was taken from Pegah Dairy Company (Tehran, Iran) and the effect of operational parameters, including adsorbent dose, pH, and contact time were studied on the removal of total nitrogen, total phosphorus, COD, and turbidity. In Situ Sludge Magnetic Impregnation" (ISSMI) was used for sludge separation after adsorption process. To increase the interaction between the magnetic nanoparticles and graphene oxide, surface of magnetic nanoparticles was modified with amine functional group. SEM, FT-IR, CHNS, and VSM analysis confirmed that GO and magnetic nanoparticles had been prepared properly. High adsorption capacity, high adsorption rate, and high sludge separation rate were some of the significant features of the proposed treatment process. By increasing GO dose,

TN, TP, COD, and turbidity plummeted, and at adsorbent dose of 320 mg L^{-1}, the removal efficiencies of 90%, 80%, 84%, and 94% were observed for TN, TP, COD, and turbidity, respectively. The maximum absorption capacity of the adsorbent was 730 mg g^{-1} for total nitrogen, 600 mg g^{-1} for total phosphorus, 26000 mg g^{-1} for COD, and 5500 mg g^{-1} for turbidity. The highest removal efficiencies were obtained after 10 min of stirring. Freundlich and Temkin exhibited lower errors than Langmuir with the fitting degree following the sequence of Freundlich> Temkin > Langmuir. In dairy wastewater, TN, TP, and COD are mostly particulate materials; therefore, when GO nanosheets aggregate, particulate materials are trapped between nanosheets; therefore, pollutants are distributed heterogeneously on the surface of adsorbent. As a consequence, the adsorption does not occur as monolayer on the surface of GO. For this reason, the adsorption followed Freundlich model. The

adsorption kinetics followed the pseudo-second-order model. Regarding the short contact time, feasibility of absorption process, and elimination of sludge-related expenses, this process can appropriately substitute biological processes for nitrogen, phosphorus, COD, and turbidity removal.

Acknowledgements

REFERENCES

Ali, I., Asim, M. and Khan, T.A. (2012). Low cost adsorbents for the removal of organic pollutants from wastewater. J. Environ. Manage., 113: 170-183.

Demirel, B., Yenigun, O. and Onay, T.T. (2005). Anaerobic treatment of dairy wastewaters: a review. Process Biochem., 40: 2583-2595.

Doğan, M., Alkan, M. and Onganer, Y. (2000). Adsorption of methylene blue from aqueous solution onto perlite. Water. Air. Soil Pollut., 120: 229-248.

Drogui, P., Asselin, M., Brar, S.K., Benmoussa, H. and Blais, J.F. (2008). Electrochemical removal of pollutants from agro-industry wastewaters. Sep. Purif. Technol., 61: 301-310.

Gavala, H.N., Kopsinis, H., Skiadas, I.V., Stamatelatou, K. and Lyberatos, G. (1999). Treatment of dairy wastewater using an upflow anaerobic sludge blanket reactor. J. Agric. Eng. Res., 73: 59-63.

Geetha Devi, M., Dumaran, J.J. and Feroz, S. (2012). Dairy wastewater treatment using low molecular weight crab shell chitosan. J. Inst. Eng. Ser. E, 93; 9-14.

Hameed, B.H. (2009). Spent tea leaves: A new non-conventional and low-cost adsorbent for removal of basic dye from aqueous solutions. J. Hazard. Mater., 161: 753-759.

Hummers J.W.S. and Offeman, R.E. (1958). Preparation of graphitic oxide. J. Am. Chem. Soc., 80: 1339.

Karale, S.S. and Suryavanshi, M.M. (2014). Dairy wastewater treatment using coconut shell activated carbon & laterite as low cost adsorbents. Int. J. Civil, Struct. Environ. Infrastruct. Eng. Res. Dev., 1: 9-14.

Khosroshahi, M.E. and Ghazanfari, L. (2012). Synthesis and functionalization of SiO_2 coated Fe_3O_4 nanoparticles with amine groups based on self-assembly. Mater. Sci. Eng. C, 32: 1043-1049.

Kurniawan, A., Sutiono, H., Indraswati, N. and Ismadji, S. (2012). Removal of basic dyes in binary system by adsorption using rarasaponin-bentonite: Revisited of extended Langmuir model. Chem. Eng. J., 189-190: 264-274.

Kushwaha, J.P., Srivastava, V.C. and Mall, I.D. (2011). An overview of various technologies for the treatment of dairy wastewaters. Crit. Rev. Food Sci. Nutr., 51: 442-452.

Kushwaha, J.P., Srivastava, V.C. and Mall, I.D. (2010). Treatment of dairy wastewater by commercial activated carbon and bagasse fly ash: Parametric, kinetic and equilibrium modelling, disposal studies. Bioresour. Technol., 101: 3474-3483.

Loures, C.C.A., Filho, H.J.I., Samanamud, G.R.L., Souza, A.L., Salazar, R.F.S., Peixoto, A.L.C. and Guimarães, O.L.C. (2013). Performance evaluation of photo-fenton and fenton processses for dairy effluent treatment. Int. Rev. Chem. Eng., 5: 280.

Luo, J., Ding, L., Qi, B., Jaffrin, M.Y. and Wan, Y. (2011). A two-stage ultrafiltration and nanofiltration process for recycling dairy wastewater. Bioresour. Technol., 102: 7437-7442.

Mañas, A., Biscans, B. and Spérandio, M. (2011). Biologically induced phosphorus precipitation in aerobic granular sludge process. Water Res., 45: 3776-3786.

Manu, K.J., Mohana, V.S. and Ganeshaiah, K.N. (2011). Effluent generation by the dairy units: Characterization and amelioration for irrigation. Int J Res Chem Env., 1: 173-182.

Mitra, T., Singha, B., Bar, N. and Das, S.K. (2014). Removal of Pb(II) ions from aqueous solution using water hyacinth root by fixed-bed column and ANN modeling. J. Hazard. Mater., 273: 94-103.

Moharramzadeh, S. and Baghdadi, M. (2016). In situ sludge magnetic impregnation (ISSMI) as an efficient technology for enhancement of sludge sedimentation: Removal of methylene blue using nitric acid treated graphene oxide as a test process. J. Environ. Chem. Eng., 4: 2090-2102.

Moradi, O. and Maleki, M.S. (2013). Removal of COD from dairy wastewater by MWCNTs: adsorption isotherm modeling. Fullerenes, Nanotub. Carbon Nanostructures, 21: 836-848.

Murali, K., Karuppiah, P.L., Nithish, M., Kumar, S.S. and Raja, V.S. (2013). COD reduction using low cost biosorbent as part of cleaner production. Int. J. Sci. Res. Publ., 3: 1-3.

Omidinia, E., Shadjou, N. and Hasanzadeh, M. (2013). (Fe$_3$O$_4$)-graphene oxide as a novel magnetic nanomaterial for non-enzymatic determination of phenylalanine. Mater. Sci. Eng. C, 33: 4624-4632.

Porwal, H.J., Mane, A.V. and Velhal, S.G. (2015). Biodegradation of dairy effluent by using microbial isolates obtained from activated sludge. Water Resour. Ind., 9: 1-15.

Rahimi, Y., Torabian, A., Mehrdadi, N., Habibi-Rezaie, M., Pezeshk, H. and Nabi-Bidhendi, G.R. (2011). Optimizing aeration rates for minimizing membrane fouling and its effect on sludge characteristics in a moving bed membrane bioreactor. J. Hazard. Mater., 186: 1097-1102.

Särkkä, H., Vepsäläinen, M. and Sillanpää, M. (2015). Natural organic matter (NOM) removal by electrochemical methods- A review. J. Electroanal. Chem., 755: 100-108.

Tawfik, A., Sobhey, M. and Badawy, M. (2008). Treatment of a combined dairy and domestic wastewater in an up-flow anaerobic sludge blanket (UASB) reactor followed by activated sludge (AS system). Desalination, 227: 167-177.

Weber, W.J. and Morris, J.C. (1963). Kinetics of adsorption on carbon from solution. J. Sanit. Eng. Div., 89: 31-60.

Yavuz, Y., Öcal, E., Koparal, A.S. and Öğütveren, Ü.B. (2011). Treatment of dairy industry wastewater by EC and EF processes using hybrid Fe-Al plate electrodes. J. Chem. Technol. Biotechnol., 86: 964-969.

Zhu, Y., Murali, S., Cai, W., Li, X., Suk, J.W., Potts, J.R. and Ruoff, R.S. (2010). Graphene and graphene oxide: synthesis, properties, and applications. Adv. Mater., 22: 3906-24.

Zong, P., Wang, S., Zhao, Y., Wang, H., Pan, H. and He, C. (2013). Synthesis and application of magnetic graphene/iron oxides composite for the removal of U(VI) from aqueous solutions. Chem. Eng. J., 220: 45-52.